ORIGINAL RESEARCH

Nicotinamide Adenine Dinucleotide Phosphate Oxidase 2 Regulates LPS-Induced Inflammation and Alveolar Remodeling in the Developing Lung

Heather L. Menden, Sheng Xia, Sherry M. Mabry, Angels Navarro, Michael F. Nyp, and Venkatesh Sampath

Department of Pediatrics, Division of Neonatology, Children's Mercy Hospital, Kansas City, Missouri

Abstract

In premature infants, sepsis is associated with alveolar simplification manifesting as bronchopulmonary dysplasia. The redox-dependent mechanisms underlying sepsis-induced inflammation and alveolar remodeling in the immature lung remain unclear. We developed a neonatal mouse model of sepsis-induced lung injury to investigate whether nicotinamide adenine dinucleotide phosphate oxidase 2 (NOX2) regulates Toll-like receptor (TLR)–mediated inflammation and alveolar remodeling. Six-day-old $NOX2^{+/+}$ and $NOX2^{-/-}$ mice were injected with intraperitoneal LPS to induce sepsis. Lung inflammation and canonical TLR signaling were assessed 24 hours after LPS. Alveolar development was examined in 15-day-old mice after LPS on Day 6. The *in vivo* efficacy of a NOX2 inhibitor (NOX2-I) on NOX2 complex assembly and sepsis-induced lung inflammation were examined. Lung cytokine expression and neutrophil influx induced with sepsis in $NOX2^{+/+}$ mice was decreased by >50% in $NOX2^{-/-}$ mice. LPS-induced TLR4 signaling evident by inhibitor of NF-κB kinase-β and mitogen-activated protein kinase phosphorylation, and nuclear factor-κB/AP-1 translocation were attenuated in $NOX2^{-/-}$ mice. LPS increased matrix metalloproteinase 9 while decreasing elastin and keratinocyte growth factor levels in $NOX2^{+/+}$ mice. An LPS-induced increase in matrix metalloproteinase 9 and decrease in fibroblast growth factor 7 and elastin were not evident in $NOX2^{-/-}$ mice. An LPS-induced reduction in radial alveolar counts and increased mean linear intercepts were attenuated in $NOX2^{-/-}$ mice. LPS-induced NOX2 assembly evident by p67*phox*/gp91*phox* coimmunoprecipitation was disrupted with NOX2-I. NOX2-I also mitigated LPS-induced cytokine expression, TLR pathway signaling, and alveolar simplification. In a mouse model of neonatal sepsis, NOX2 regulates proinflammatory TLR signaling and alveolar remodeling induced by a single dose of LPS. Our results provide mechanistic insight into the regulation of sepsis-induced alveolar remodeling in the developing lung.

Keywords: nicotinamide adenine dinucleotide phosphate oxidase; sepsis; Toll-like receptor signaling; neonatal lung injury; bronchopulmonary dysplasia

Postnatal inflammation and tissue injury in the developing lung contribute to the disrupted alveolar development observed in premature infants with bronchopulmonary dysplasia (BPD) (1, 2). Risk factors associated with BPD, such as hyperoxia, barotrauma, and sepsis, trigger the production of reactive oxygen species (ROS) in the premature lung, which contributes to lung inflammation and matrix degradation (3–5). Multiple investigators have shown that markers of oxidant-mediated lung injury, such as 8-Oxo-2′-deoxyguanosine, oxidized surfactant phospholipids, F2-isoprostanes, and nitrotyrosine, are elevated in the bronchoalveolar lavage, serum, or urine of premature infants who subsequently develop BPD (4–7). Therapies to mitigate oxidant stress, such as recombinant superoxide dismutase and vitamin A, have been used in premature infants to decrease BPD, with limited success (8, 9). The preterm infant lung is particularly vulnerable to oxidant-mediated damage because lung antioxidant enzymes are

Clinical Relevance

Our data provide mechanistic insight into sepsis-induced alveolar remodeling seen in premature infants with bronchopulmonary dysplasia. We demonstrate that nicotinamide adenine dinucleotide phosphate oxidase 2 regulates sepsis-induced inflammatory signaling and alveolar simplification in the developing lung. Use of a peptide inhbitor of nicotinamide adenine dinucleotide phosphate oxidase 2 during sepsis attenuates neonatal lung injury, suggesting a potential therapy for neonatal lung protection during sepsis.

developmentally regulated and not fully functional until term gestation (3, 6). Gram-negative bacterial sepsis is a common complication of preterm birth and is associated with an acute increase in ROS, lung inflammation, and the development of BPD (10, 11). The redox-dependent mechanisms regulating sepsis-induced inflammation and alveolar remodeling in the developing lung remain poorly understood and are the focus of this study.

During sepsis, bacterial cell-wall components such as LPS are recognized by the Toll-like receptor (TLR) family of innate immune receptors (12, 13). TLR-mediated bacterial recognition triggers complex signaling cascades, resulting in the activation of transcription factors nuclear factor-κB (NF-κB) and AP-1, which regulate inflammation and tissue injury in the lung (12). Activation of canonical TLR signaling increases intracellular ROS, and TLR-mediated inflammation has been shown *in vitro* to be regulated by the nicotinamide adenine dinucleotide phosphate oxidase (NOX) enzymes (14–17). The NOX family of oxidoreductases generates superoxide by one electron reduction of molecular oxygen using the reduced form of nicotinamide adenine dinucleotide phosphate+ as substrate. The seven NOX catalytic homologs differ in subunit composition, tissue distribution, and mode of activation (14, 16). Some NOX isoforms, such as NOX4, are constitutively active, whereas others are activated by cellular stress, hormones, cytokines, and bacterial ligands. NOX-derived ROS play a key role in homeostatic cellular

signaling when compartmentalized and regulated (16, 18). However, pathological activation of NOX has been implicated in various disease processes such as ischemia-reperfusion, inflammation, hypertension, and cancer (14, 18). In the lung, NOX isoforms show cell-type–specific distribution and function and are found in endothelial cells, epithelial cells, fibroblasts, macrophages, and smooth muscle cells (18). Prior work in our laboratory demonstrated that nicotinamide adenine dinucleotide phosphate oxidase 2 (NOX2) regulates LPS (TLR4 agonist)–mediated superoxide production and cytokine expression in fetal lung endothelial cells (15). To determine the *in vivo* relevance of NOX2 in proinflammatory TLR signaling, we used a mouse model to investigate whether NOX2 regulated sepsis-induced inflammation and alveolar remodeling in the developing lung.

Lung development in rodents is similar to that in premature infants because it progresses through the saccular and alveolar phase after birth (19). Traditionally, rodent models of BPD have used hyperoxia, antenatal endotoxin exposure, and mechanical ventilation to induce acute lung inflammation and alveolar remodeling in the immature lung (20, 21). Although it is accepted that systemic sepsis in the premature infant is a major risk factor for the development of BPD, the mechanisms by which sepsis-induced acute lung inflammation contributes to alveolar simplification in BPD remain poorly understood (11, 22, 23). To investigate the mechanisms underlying sepsis-induced inflammation and alveolar remodeling in the immature lung, we developed a model of neonatal sepsis using intraperitoneal LPS administration in 6-day-old mouse pups. We hypothesized that LPS-induced acute lung inflammation would remodel the developing lung and that NOX2 deficiency would protect against TLR-mediated lung injury. The results of this study suggest that NOX2 regulates sepsis-mediated lung inflammation and alveolar remodeling in the developing lung.

Materials and Methods

Animal Model
Care of mice before and during experimental procedures was performed

in accordance with the policies of the Biomedical Resource Center, Medical College of Wisconsin, Laboratory Animal Research Core, University of Missouri–Kansas City, and the National Institutes of Health guidelines for the care and use of laboratory animals. All protocols had prior approval from the Medical College of Wisconsin Institutional Animal Care and Use Committee (AUA 3464) and the University of Missouri–Kansas City Institutional Animal Care and Use Committee (protocol number 1510). In experiments using the $NOX2^{-/-}$ animal model, timed breeding was used for animal comparisons. When the pups were at Day of Life 6, they received intraperitoneal injection of 1 mg/kg LPS (Sigma, St. Louis, MO), whereas the control mice received an equal volume injection of sterile saline solution. The pups were killed at 3, 6, 24, 96, or 196 hours after LPS administration using an intraperitoneal injection of a ketamine and xylazine mixture (100 mg/kg, 10 mg/kg, respectively). For experiments with the NOX2 inhibitor, gp91*phox* ds-*tat* (10 mg/kg, NOX2-inhibitor [NOX2-I]; Anaspec, Fremont, CA), and the p38 inhibitor SB202190 (10 mg/kg, p38-I; Abcam, Cambridge, MA), drugs were injected intraperitoneally 2 hours before intraperitoneal LPS injection. Lungs were harvested and used for experimentation as described below.

Hematoxylin and Eosin Staining to Assess Lung Development in Inflated Mouse Lungs
$NOX2^{+/+}$ and $NOX2^{-/-}$ mouse pups were killed 196 hours after intraperitoneal injection of LPS or saline. The lungs were inflated using a fixed volume of formalin, as described previously by Parkinson and colleagues (24). Briefly, using a catheter, 300 μL of formalin fixative was used to inflate the lungs after the mice were killed. Precautions were taken to not over- or underinflate the lungs. The lungs were further fixed in formalin before being embedded in paraffin, cut into 4-μm sections onto slides, and stained with hematoxylin and eosin. The hematoxylin and eosin slides were scanned using a NanoZoomer slide scanner (Hamamatsu, Bridgewater, NJ), and the scanned

images were used at 40× for assessing radial alveolar count (25) and mean linear intercepts (26) following previously used protocols. At least four mice were used per condition in these experiments. For radial alveolar counts, quantification was performed by averaging 10 measurements per mouse. For mean linear intercepts, quantifications were performed by averaging five high-power fields per mouse.
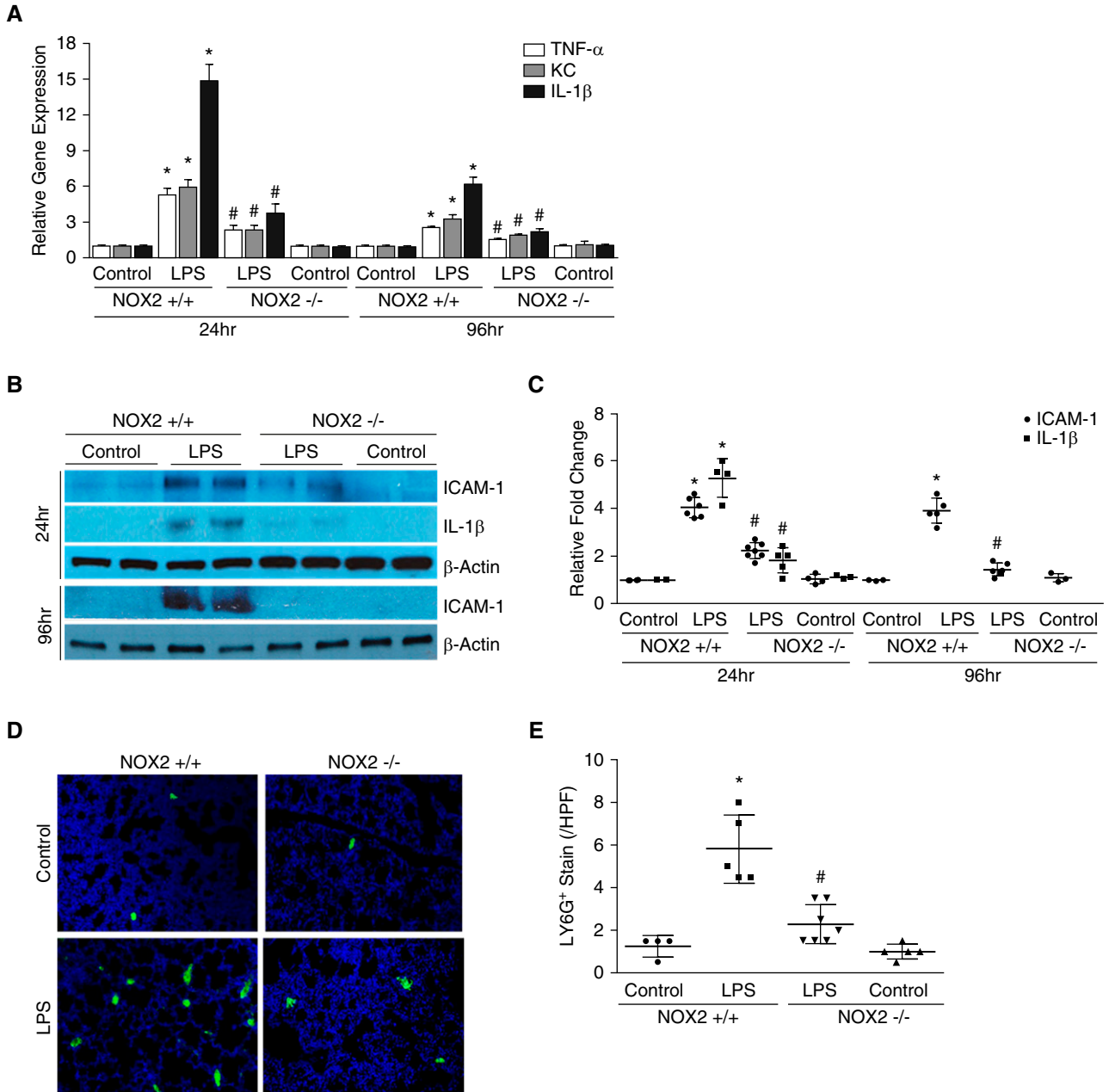

Figure 1. Lung cytokine expression and neutrophil influx after intraperitoneal (i.p.) LPS injection. Six-day-old nicotinamide adenine dinucleotide phosphate oxidase 2 (NOX2)$^{+/+}$ and NOX2$^{-/-}$ pups were injected intraperitoneally with LPS or saline, and the lungs were harvested for real-time polymerase chain reaction and protein analysis at 24 and 96 hours (A–C). The left lung was used for immunofluorescence studies (D–E). (A) TNF-α, keratinocyte-derived cytokine (KC), and IL-1β mRNA expression quantified by real-time polymerase chain reaction after intraperitoneal LPS injections. *$P < 0.01$ (NOX2$^{+/+}$ control versus NOX2$^{+/+}$ i.p. LPS); #$P < 0.02$ (NOX2$^{+/+}$ i.p. LPS versus NOX2$^{-/-}$ i.p. LPS) ($n = 5$). (B and C) Homogenized lung lysates after intraperitoneal injections of LPS in mouse pups were immunoblotted for intercellular adhesion molecule (ICAM-1) and IL-1β (B), with densitometric quantification of ICAM-1 and IL-1β shown graphically (C). *$P < 0.01$ (NOX2$^{+/+}$ control versus NOX2$^{+/+}$ i.p. LPS); #$P < 0.02$ (NOX2$^{+/+}$ i.p. LPS versus NOX2$^{-/-}$ i.p. LPS) ($n = 5$). (D) Fluorescent microscope images depicting neutrophil influx by LY6G immunofluorescence staining. LY6G is shown in *green* and DAPI in *blue*. Images are shown at 20× magnification. (E) Graphical representation summarizing the data, with each mouse shown as an average of three representative images. *$P < 0.05$ (NOX2$^{+/+}$ control versus NOX2$^{+/+}$ i.p. LPS); #$P = 0.01$ (NOX2$^{+/+}$ i.p. LPS versus NOX2$^{-/-}$ i.p. LPS) ($n \geq 4$). ANOVA with *post hoc* tests was used for analysis of data. HPF, high-powered field.

Treatment of Mice with gp91 ds-*tat* (NOX2-I) and SB202190 (p38-I) Chemical Injections

Two hours before intraperitoneal injection of LPS/saline, NOX2$^{+/+}$ mouse pups were pretreated with intraperitoneal injection of 10 mg/kg of NOX2-I or p38-I or saline. Mice were killed 24 hours after the NOX2-I or p38-I injection, and harvested lung lobes were used for RNA (complementary DNA, real-time polymerase chain reaction) isolation and protein (Western blot) quantification, as described above. At least four mice were used per experimental condition.
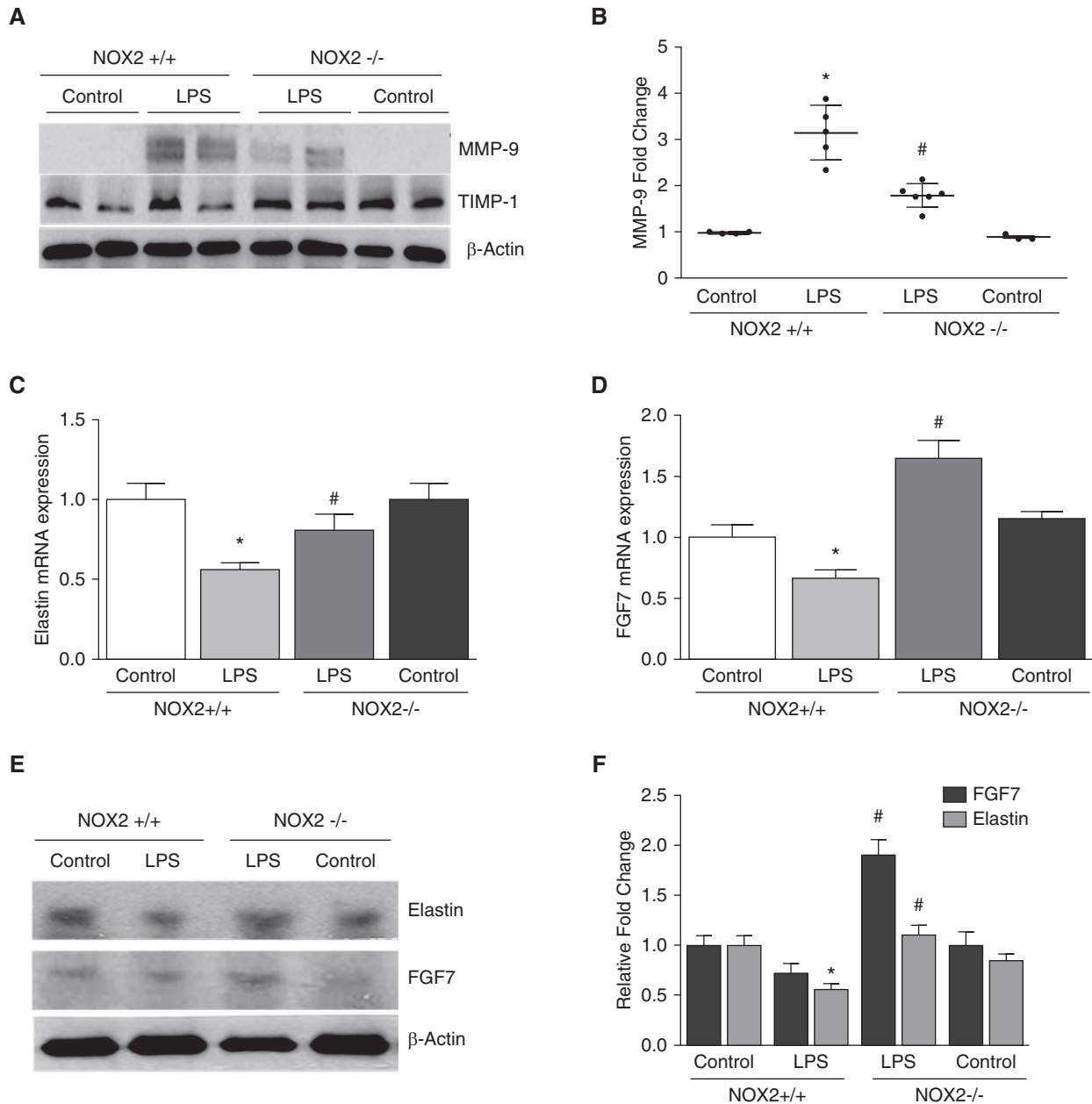

Figure 2. Lung matrix metalloproteinase 9 (MMP-9), tissue inhibitor of matrix metalloproteinase 1 (TIMP-1), elastin, and keratinocyte growth factor 7 expression after intraperitoneal LPS injection. Lungs were harvested from NOX2$^{+/+}$ and NOX2$^{-/-}$ mouse pups injected with intraperitoneal LPS or saline after 24 or 96 hours for protein analysis. (A) Homogenized lung lysates were used to immunoblot MMP-9 and TIMP-1 at 24 hours; β-actin was used as a loading control. (B) MMP-9 quantification by densitometry is shown graphically. *$P < 0.01$ (NOX2$^{+/+}$ control versus NOX2$^{+/+}$ i.p. LPS); #$P < 0.01$ (NOX2$^{+/+}$ i.p. LPS versus NOX2$^{-/-}$ i.p. LPS) ($n \geqslant 4$). (C and D) Elastin (C) and fibroblast growth factor 7 (FGF7) (D) mRNA expression was quantified by real-time polymerase chain reaction 96 hours after intraperitoneal LPS injection. *$P < 0.05$ (NOX2$^{+/+}$ control versus NOX2$^{+/+}$ i.p. LPS); #$P < 0.02$ (NOX2$^{+/+}$ i.p. LPS versus NOX2$^{-/-}$ i.p. LPS) ($n \geqslant 4$). (E and F) Clarified lung lysates obtained 96 hours after LPS treatment in pups were blotted for FGF7 and elastin (E), with quantification by densitometry shown graphically (F). *$P < 0.01$ (NOX2$^{+/+}$ control versus NOX2$^{+/+}$ i.p. LPS); #$P = 0.01$ (NOX2$^{+/+}$ i.p. LPS versus NOX2$^{-/-}$ i.p. LPS) ($n \geqslant 4$). ANOVA with *post hoc* tests was used for analysis of data.

Supplement Section

Experimental detail for polymerase chain reaction, immunoblotting, phosphorylation, electrophoretic mobility shift assay, coimmunoprecipitation, and immunofluorescence studies, as well as data analysis, are presented in the online supplement.

Results

NOX2 Regulates LPS-Mediated Acute Inflammation in the Developing Lung

We examined the effect of NOX2 deficiency on lung inflammation induced by intraperitoneal LPS injection in 6-day-old mice. Whole-lung TNF-α, keratinocyte-derived cytokine (KC), and IL-1β RNA expressions were increased more than fourfold at 24 and 96 hours after intraperitoneal LPS (Figure 1A). LPS-mediated increase in inflammatory gene expression was attenuated by ~50% in NOX2$^{-/-}$ mice (Figure 1A). Similarly, whole-lung protein expression of intercellular adhesion molecule (ICAM-1), which facilitates lung neutrophil influx, and IL-1β induced with systemic LPS were attenuated in NOX2$^{-/-}$ mice (Figures 1B and 1C). These data reveal that deficiency of NOX2 attenuates the pulmonary expression of proinflammatory cytokines induced with systemic LPS in 6-day-old mice. Neutrophil influx is a prominent feature of acute lung injury that contributes to lung inflammation and matrix degradation. To evaluate the effect of NOX2 deficiency on LPS-mediated lung neutrophil invasion, we performed immunofluorescence for Ly6G (a specific marker for neutrophils) in 4-μM lung sections 24 hours after intraperitoneal LPS. LPS-induced lung neutrophil influx at 24 hours was decreased by >60% in NOX2$^{-/-}$ mice (Figures 1 D and 1E). These data demonstrate that the lung inflammation and neutrophil influx observed with systemic LPS is attenuated in NOX2$^{-/-}$ mice.

Effect of NOX2 Deficiency on Markers of Matrix Remodeling and Lung Growth

To evaluate the effect of sepsis on matrix degradation in the developing lung, we assessed protein levels of matrix metalloproteinase (MMP) 9 (MMP-9) and the tissue inhibitor of matrix

metalloproteinase (TIMP) 1 (TIMP-1) after intraperitoneal LPS in 6-day-old mice. LPS administration induced lung MMP-9 levels by more than threefold at 24 hours (Figures 2A and 2B). Lung TIMP-1 expression was evident in control NOX2$^{+/+}$ mice and remained unchanged after intraperitoneal LPS (Figure 2A). In NOX2$^{-/-}$ mice, LPS-induced lung MMP-9 expression was attenuated by >40% (Figures 2A and 2B) when compared with NOX2$^{+/+}$ mice. Lung TIMP-1 expression in control NOX2$^{-/-}$ mice showed a nonsignificant increase when compared with NOX2$^{+/+}$ mice but did not change with systemic LPS. These data suggest decreased MMP-9–dependent remodeling with sepsis in NOX2$^{-/-}$ mice.

To examine the effect of systemic LPS on pathways related to alveolar growth, we quantified Keratinocyte growth factor (fibroblast growth factor 7 [FGF7]), a lung growth factor, and elastin (27, 28). There

were no significant changes in elastin and FGF7 RNA or protein 24 hours after LPS in NOX2$^{+/+}$ mice (data not shown), but both RNA and protein expression of elastin and FGF7 were reduced at 96 hours after LPS (Figures 2C–2E). The LPS-induced decrease in lung elastin RNA and protein expression was attenuated in NOX2$^{-/-}$ mice (Figures 2C–2E). Interestingly, systemic LPS appeared to induce FGF7 protein in NOX2$^{-/-}$ mice, resulting in significantly higher lung FGF7 levels when compared with NOX2$^{+/+}$ mice treated with LPS. These data suggest that markers of lung growth are decreased with LPS in NOX2$^{+/+}$ mice but are preserved in NOX2$^{-/-}$ mice.

NOX2 Regulates Pulmonary TLR Pathway Activation in Sepsis

To investigate the mechanisms by which NOX2 regulates sepsis-induced inflammation in the developing lung, we
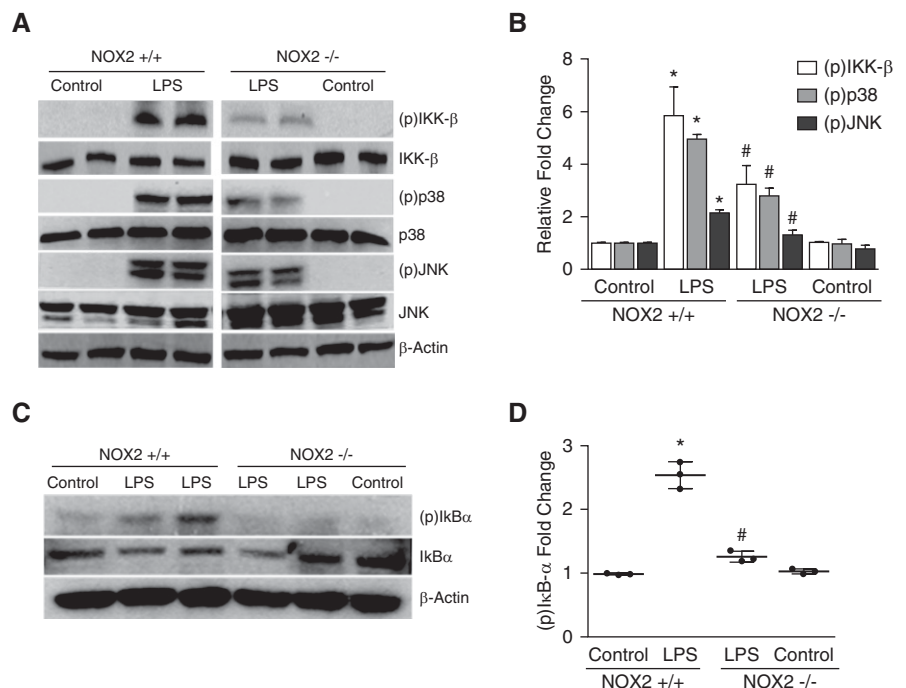
Figure 3. Changes in inhibitor of NF-κB kinase-β (IKK-β), p38, c-Jun N-terminal kinase (JNK), and inhibitor of NF-κB-α (IκB) phosphorylation after LPS injection: Six-day-old NOX2$^{+/+}$ and NOX2$^{-/-}$ mouse pups were exposed to intraperitoneal injections of LPS or saline, and the lungs were harvested for Western blot. (*A* and *B*) Mouse lung lysates were used to assess IKK-β, p38, and JNK phosphorylation 24 hours after intraperitoneal LPS treatment by immunoblotting (*A*), and blots were quantified by densitometry (*B*). *$P < 0.01$ (NOX2$^{+/+}$ control versus NOX2$^{+/+}$ i.p. LPS); #$P < 0.01$ (NOX2$^{+/+}$ i.p. LPS versus NOX2$^{-/-}$ i.p. LPS) ($n \geqslant 4$). (*C* and *D*) Western blot (*C*) of mouse lung lysates showing changes in IκB-α phosphorylation 24 hours after intraperitoneal injection of LPS, and graphical representation (*D*) summarizing quantification by densitometry of IκB-α phosphorylation. *$P < 0.001$ (NOX2$^{+/+}$ control versus NOX2$^{+/+}$ i.p. LPS); #$P < 0.01$ (NOX2$^{+/+}$ i.p. LPS versus NOX2$^{-/-}$ i.p. LPS) ($n \geqslant 4$). ANOVA with *post hoc* tests was used for analysis of data.

examined the effect of NOX2 deficiency on LPS-mediated canonical TLR4 pathway signaling. Systemic LPS administration robustly increased inhibitor of NF-κB kinase-β (IKK-β) phosphorylation (Ser$^{177/181}$) in the lungs of 6-day-old mice, indicating TLR pathway activation (Figures 3A and 3B). LPS-mediated IKK-β phosphorylation was inhibited by >50% in NOX2$^{-/-}$ mice (Figures 3A and 3B). Activation of the mitogen-activated protein kinase (MAPK) p38 and c-Jun N-terminal kinase (JNK) through phosphorylation is a key event that contributes to TLR-mediated inflammation. In NOX2$^{+/+}$ mice, intraperitoneal LPS-induced lung phosphorylation of p38 (Thr^{180}/Tyr^{182}) and JNK (Thr^{183}/Tyr^{185}) was evident at 24 hours (Figures 3A and 3B). p38 and JNK phosphorylation induced by systemic LPS were decreased in the lungs of NOX2$^{-/-}$ mice. To examine the role of p38 in enhancing NF-κB signaling in our model, we performed additional experiments with the specific p38 inhibitor (p38-I, SB202190, 10 mg/kg) (29, 30). Pretreatment with p38-I (2 hr) decreased LPS-induced p38 (Thr^{180}/Tyr^{182}) phosphorylation, NF-κB activation. and proinflammatory cytokine expression in NOX2+/+ mice (see online supplement).

In canonical TLR signaling, IKK-β phosphorylation mediates inhibitor of NF-κB-α (IκB-α) phosphorylation and ubiquitination, with subsequent release and nuclear translocation of IκB-bound NF-κB. To examine IκB-α cellular dynamics in our model, we examined IκB-α phosphorylation after systemic LPS. Lung IκB-α (Ser^{32}) phosphorylation was increased with intraperitoneal LPS in NOX2$^{+/+}$ mice at 20 hours (Figures 3C and 3D). NOX2 deficiency attenuated the IκB-α (Ser^{32}) phosphorylation seen with systemic LPS treatment (Figures 3C and 3D). These results suggest that NOX2 regulates TLR pathway kinase activation and IκB-α phosphorylation during sepsis in the developing lung.

LPS-Mediated Lung NF-κB and AP-1 Activation Is Attenuated in NOX2$^{-/-}$ Mice

Activation of the transcription factors NF-κB and AP-1in the lung during sepsis regulates proinflammatory cytokine expression (10). We therefore evaluated lung NF-κB and AP-1 activation in 6-day-old mice by quantifying nuclear translocation of the p65 and c-Jun subunits, respectively, using immunofluorescence.

Twenty-four hours after systemic LPS, there was increased nuclear staining of p65 (Figures 4A and 4C) and c-Jun (Figures 4B and 4C) in lung sections. The number of lung cells with nuclear staining of p65 and c-Jun after LPS was attenuated in NOX2$^{-/-}$ mice (Figures 4A–4C). These data indicate that activation of NF-κB and

AP-1 with sepsis is NOX2 dependent in the developing lung. To confirm NF-κB activation after LPS, we performed a shift assay for p65 in whole-lung nuclear homogenates. After LPS treatment, there was increased p65 in NOX2$^{+/+}$ lung nuclear extracts, which was attenuated in NOX2$^{-/-}$ mice (Figures 4D and 4E).
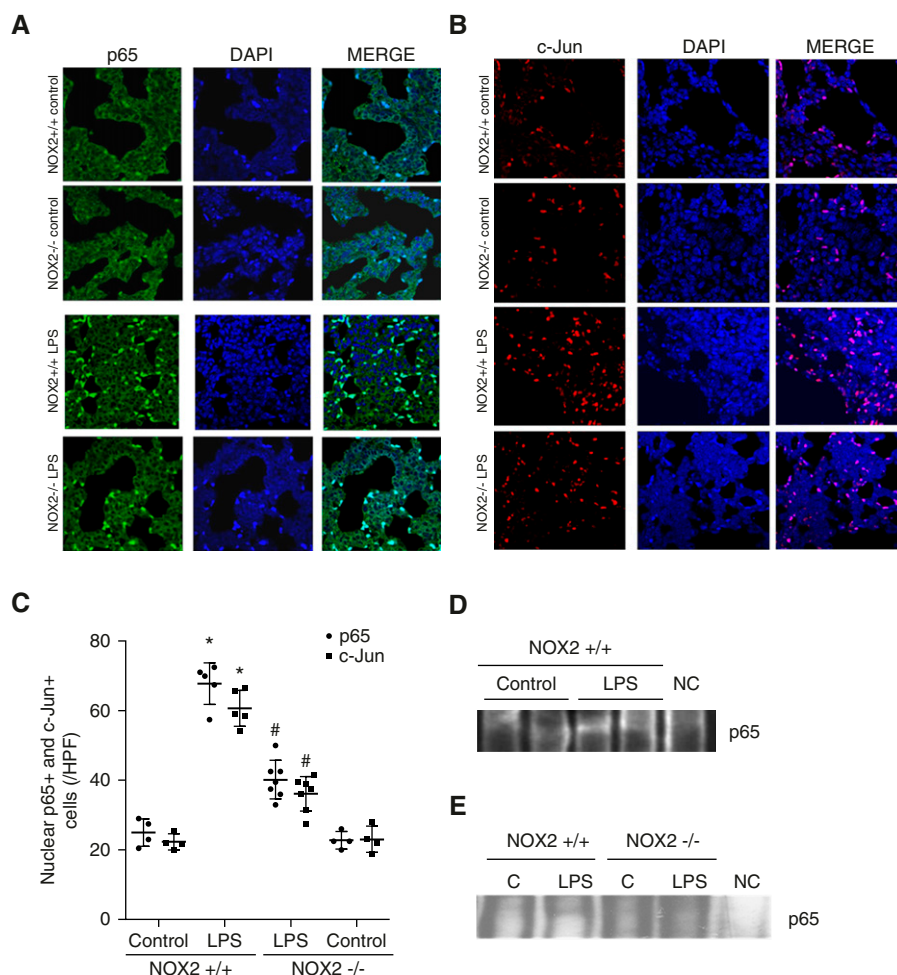

Figure 4. Assessment of NF-κB (p65) and AP-1 (c-Jun) activation after intraperitoneal LPS injection. Lung sections (4 μM) obtained from 6-day-old NOX2$^{+/+}$ and NOX2$^{-/-}$ mouse pups 24 hours after treatment with LPS or saline were used for immunofluorescence studies. Lung nuclear extracts obtained from pups 3 hours after treatment with LPS or saline were used for electrophoretic mobility shift assay. (A) Confocal microscope images depicting nuclear activation of p65 by immunofluorescence staining. p65 in the cytoplasm stains *green* and DAPI (nucleus) is *blue*; the *light blue* staining is activated p65 in the nucleus. Images were captured at 63× magnification. (B) Confocal microscope images depicting nuclear activation of c-Jun by immunofluorescence staining. c-Jun in the cytoplasm stains *red* and DAPI is *blue*; the *magenta* staining is activated c-Jun in the nucleus. Images are shown at 63× magnification. (C) Graphical representation summarizing data of nuclear p65 and c-Jun, with each mouse shown as an average of three representative images. *P < 0.01 (NOX2$^{+/+}$ control versus NOX2$^{+/+}$ i.p. LPS); #P < 0.01 (NOX2$^{+/+}$ i.p. LPS versus NOX2$^{-/-}$ i.p. LPS) (n ≥ 4). (D and E) Lung nuclear extracts were used with an electrophoretic mobility shift assay using NF-κB (p65) binding oligo. A gel-shifted band appears in LPS-treated NOX2$^{+/+}$ lungs (D and E), but not NOX2$^{-/-}$ lungs (E). There was no band present in the negative control (NC), which had a combination of hot and cold probes. C, control.

Effect of NOX2 ds-*tat* on LPS-Induced Lung Inflammation and TLR Signaling

To investigate the therapeutic potential of NOX2 activity modulation in sepsis-induced lung inflammation, we tested intraperitoneal gp91*phox* ds-*tat* (NOX2-I, 10 mg/kg), a synthetic peptide that binds to gp91*phox* and inhibits NOX2 assembly in our model (31). First, we examined the assembly of NOX2 complex in the lung by immunoprecipitating gp91*phox* and probing for the cytosolic subunit p67*phox*. In control NOX2$^{+/+}$ mice, p67*phox* was not bound to gp91*phox*. LPS treatment induced the association of p67*phox* with gp91*phox* in whole-lung homogenates, suggesting activation of NOX2 complex assembly (Figure 5A). LPS-induced lung NOX2 assembly was inhibited in mice pretreated (2 hr) with intraperitoneal NOX2-I (Figures 5A and 5B). Consistent with inhibition of lung NOX2 complex formation with NOX2-I, LPS-induced lung cytokine RNA expression and ICAM-1 expression at 24 hours were attenuated in mice pretreated with intraperitoneal NOX2-I (Figures 5C–5E). These data show that NOX2 inhibition ameliorates LPS-induced inflammation in the developing lung.

We next examined whether NOX2-I inhibits proinflammatory TLR signaling in 6-day-old mice. LPS-induced IKK-β (Ser$^{177/181}$), p38 (Thr^{180}/Tyr^{182}), and JNK (Thr^{183}/Tyr^{185}) phosphorylation in the lung was attenuated in mice pretreated with intraperitoneal NOX2-I (Figures 6A and 6B). Similarly, LPS-induced lung NF-κB activation examined by quantifying p65 nuclear translocation 24 hours after LPS was also decreased in mice pretreated with NOX2-I (Figures 6C and 6D). These data show that NOX2-I mitigates LPS-induced inflammation in the developing lung by modulating proinflammatory TLR signaling.

Effect of NOX2 Deficiency on LPS-Mediated Pulmonary Alveolar Remodeling

To evaluate the impact of systemic LPS on lung development, we assessed mean radial alveolar counts and mean linear intercepts on Postnatal Day 15 after administering intraperitoneal LPS on Postnatal Day 6. Compared with control mice, LPS-treated mice had a 50% decrease in mean radial alveolar counts and a 40% increase in mean
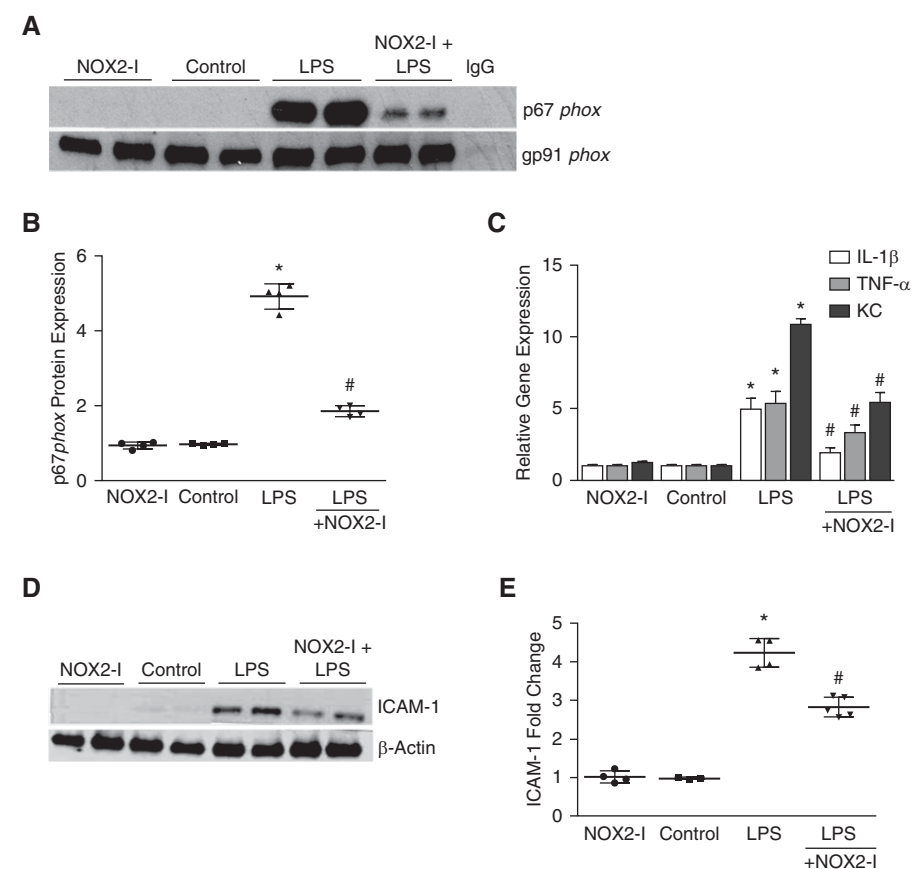
Figure 5. Effect of gp91*phox* ds-*tat* (NOX2 inhibitor [NOX2-I]) on lung NOX2 complex assembly and inflammation after intraperitoneal LPS injection. Six-day-old NOX2$^{+/+}$ mouse pups were pretreated with intraperitoneal NOX2-I (10 mg/kg) 2 hours before intraperitoneal injection of LPS or saline. (A and B) Homogenized lung lysates obtained 6 hours after intraperitoneal LPS or saline injection were immunoprecipitated for gp91*phox*, followed by Western blotting for p67*phox* and gp91*phox* (A), analysis by densitometry shown (B). *P < 0.01 (control versus i.p. LPS); #P = 0.01 (i.p. LPS versus NOX2-I + i.p. LPS) (n ≥ 4). (C) Homogenized lung lysates were used to quantify TNF-α, KC, and IL-1β mRNA expression by real-time polymerase chain reaction 24 hours after intraperitoneal injection of NOX2-I. *P < 0.01 (control versus i.p. LPS); #P < 0.05 (i.p. LPS versus NOX2-I + i.p. LPS) (n ≥ 4). (D and E) Twenty-four hours after intraperitoneal injection of LPS or saline, mouse pup lungs were homogenized, and the clarified lysates were immunoblotted for ICAM-1 (D); densitometric quantification shown graphically (E). *P < 0.01 (control versus i.p. LPS); #P < 0.05 (i.p. LPS versus NOX2-I + i.p. LPS) (n ≥ 4). ANOVA with *post hoc* tests was used for analysis of data.

linear intercepts (Figure 7). These data are supportive of disrupted lung development with LPS treatment. Because NOX2 deficiency attenuates lung inflammation after intraperitoneal LPS in our model, we investigated whether less lung inflammation in NOX2$^{-/-}$ mice translated into improved lung development. In NOX2$^{-/-}$ mice treated with LPS, mean radial alveolar counts were significantly higher, whereas mean linear intercepts were lower when compared with NOX2$^{+/+}$ mice (Figure 7). To investigate the therapeutic potential of inhibiting NOX2 in preventing sepsis-induced alveolar remodeling, we

tested NOX2-I. NOX2$^{+/+}$ mice pretreated with NOX2-I had less alveolar simplification when compared with NOX2$^{+/+}$ mice after LPS treatment (Figure 7). These data suggest that NOX2 deficiency protects against LPS-mediated alveolar remodeling in the developing lung.

Discussion

The key molecular players that regulate sepsis-induced inflammation and alveolar remodeling in the developing lung remain poorly understood. The results of this study
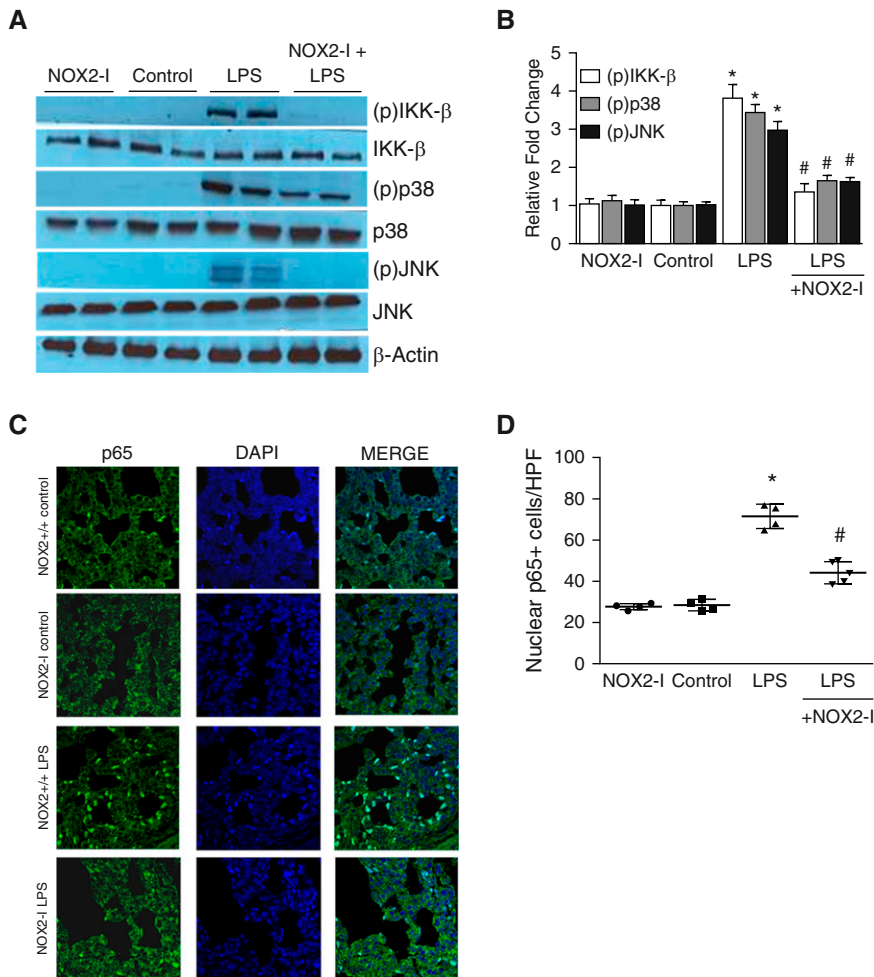
Figure 6. Effect of gp91*phox* ds-*tat* (NOX2-I) on lung Toll-like receptor pathway signaling and NF-κB activation after intraperitoneal LPS injection. Six-day-old NOX2$^{+/+}$ mouse pups were pretreated with intraperitoneal NOX2-I (10 mg/kg) 2 hours before intraperitoneal injection of LPS or saline. (*A* and *B*) Homogenized lung lysates obtained 24 hours after intraperitoneal LPS injection were used to assess the phosphorylation of IKK-β, p38, and JNK by immunoblotting (*A*), and blots were quantified by densitometry (*B*). *$P < 0.01$ (control versus i.p. LPS); #$P < 0.01$ (i.p. LPS versus NOX2-I + i.p. LPS) ($n \geqslant 4$). (*C* and *D*) Confocal microscope images depicting nuclear activation of NF-κB (p65) by immunofluorescent staining (*C*). p65 is shown in *green* and DAPI (nucleus) is *blue*; the *light blue* staining represents cells with p65 in the nucleus, suggesting NF-κB activation. (*D*) Graph summarizing nuclear NF-κB (p65) data, with each mouse shown as an average of three representative images. *$P < 0.01$ (NOX2$^{+/+}$ control versus NOX2$^{+/+}$ i.p. LPS); #$P < 0.01$ (NOX2$^{+/+}$ i.p. LPS versus NOX2$^{-/-}$ i.p. LPS). Images were captured at 63× magnification ($n \geqslant 4$). ANOVA with *post hoc* tests was used for analysis.

establish that NOX2 regulates lung inflammation in response to systemic LPS in neonatal mice. Using both genetic and peptide-inhibitor strategies, we show that TLR signaling through the IKK-β/NF-κB and MAPK/AP-1 pathways in sepsis is regulated by NOX2. Sepsis-induced cytokine expression, neutrophil influx, and alterations in markers of lung growth/matrix remodeling were attenuated with NOX2 deficiency. We also show that sepsis-induced inflammation in late

saccular/early alveolar lung can disrupt lung development, resulting in alveolar simplification akin to that observed in premature infants who develop BPD in relation to systemic sepsis. NOX2 inhibition or deficiency attenuated sepsis-induced alveolar remodeling in the immature lung. Although our results provide novel insights into the mechanisms underlying sepsis-induced alveolar remodeling in the developing lung, lack of cell-type–specific data is a limitation of the study.

An acute increase in lung cytokine levels and neutrophil influx have been reported in infants or adults with sepsis-induced acute lung injury (10, 18, 32). In our neonatal model of sepsis induced by intraperitoneal LPS, we observed an acute increase in lung expression of cytokines TNF-α, KC (equivalent to human IL-8), IL-1β, and ICAM-1, similar to studies of sepsis-induced lung injury in adult rodent models. To determine whether NOX2-dependent signaling contributes to inflammation in the developing lung, we performed matched experiments in NOX2$^{-/-}$ mice lacking the catalytic subunit gp91*phox*. Sepsis-induced lung cytokine expression was attenuated by >50% in NOX2$^{-/-}$ mice. These data are consistent with the findings of Imai and colleagues (33), who showed that a deficiency in pathogen-induced oxidative stress protects against acute lung inflammation. Imai and colleagues (33) demonstrated that mice lacking p47*phox* (cytosolic subunit of NOX2) or TLR4 are protected against lung injury induced by H5N1 pulmonary infection. Although our model involved systemic LPS (a TLR4 ligand) injection, our data also suggest that TLR-mediated lung inflammation is NOX2 dependent in neonatal mice. In contrast with our data, the findings of Gao and colleagues (32), who used a model of *Escherichia coli* sepsis, showed that lung bacterial clearance decreased in parallel with increased lung polymorphonuclear sequestration in mice lacking gp91*phox* or p47*phox*. Their data suggest that lack of NOX2 potentiates neutrophil influx in sepsis, in contrast with our data showing decreased neutrophil influx in NOX2$^{-/-}$ mice. However, Gao and colleagues (32) did find that sepsis-induced microvascular permeability and injury were decreased in NOX2$^{-/-}$ mice. Differences in our results could potentially be explained by a cell-type–specific function of NOX2 and the use of live bacteria versus a selective TLR4 ligand in our study. In the study by Gao and colleagues (32), lack of neutrophilic NOX2 function inhibited bacterial clearance, which triggered macrophage inflammatory protein 2–induced neutrophil influx. However, decreased NOX2 function in endothelial cells protected against microvascular injury and ICAM-1–mediated lung neutrophil influx. Interestingly, Gao and colleagues (32) did find, as in our study, that lung ICAM-1
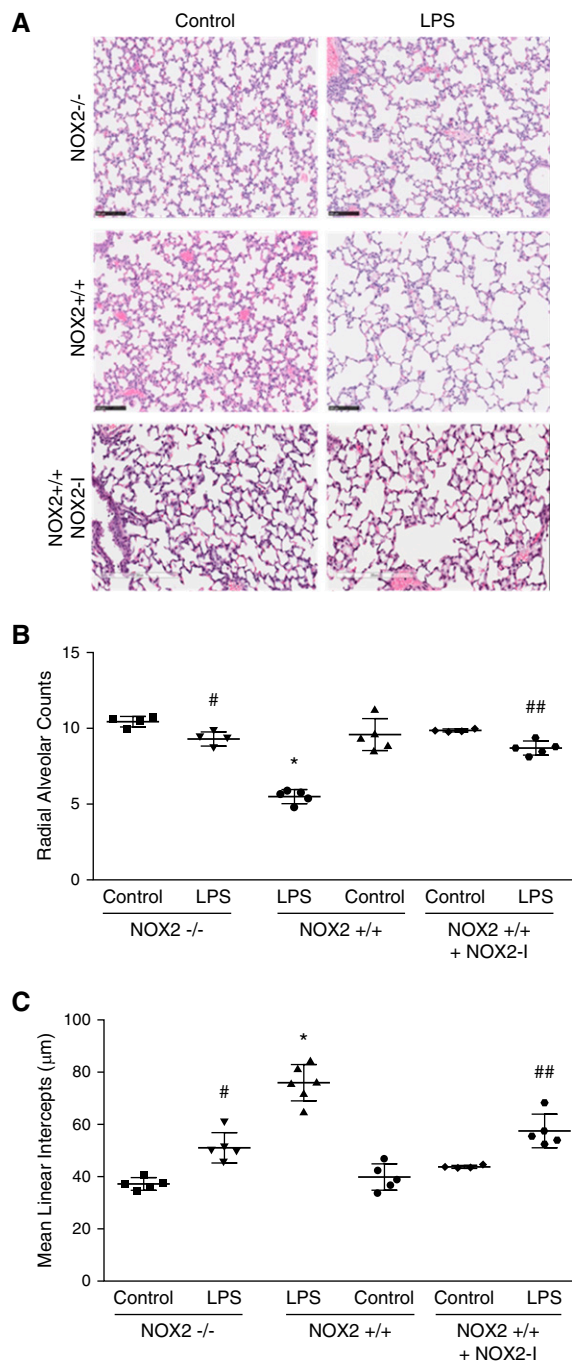
Figure 7. Changes in lung morphometry after LPS injection. NOX2$^{+/+}$, NOX2$^{-/-}$, and NOX2$^{+/+}$ pups pretreated with intraperitoneal NOX2-I were injected with LPS or saline intraperitoneally on Day of Life 6, and lungs were inflation fixed for morphometric analysis. Mouse lung sections (4 μm) were stained with hematoxylin and eosin, and pictures were scanned for analysis (A). *Scale bars*: 100 μm. (B) Radial alveolar counts were performed by averaging 10 measurements per mouse. Graphical representation summarizing radial alveolar counts is shown. *P < 0.01 (NOX2$^{+/+}$ control versus NOX2$^{+/+}$ i.p. LPS); #P < 0.01 (NOX2$^{+/+}$ i.p. LPS versus NOX2$^{-/-}$ + i.p. LPS); ##P < 0.01 (NOX2$^{+/+}$ i.p. LPS versus NOX2$^{+/+}$ + i.p. LPS + NOX2-I) (n ⩾ 4). (C) Mean linear intercepts were performed by averaging five areas per mouse. Graphical representation summarizing mean linear intercepts is shown. *P < 0.01 (NOX2$^{+/+}$ control versus NOX2$^{+/+}$ i.p. LPS); #P < 0.01 (NOX2$^{+/+}$ i.p. LPS versus NOX2$^{-/-}$ + i.p. LPS); ##P < 0.01 (NOX2$^{+/+}$ i.p. LPS versus i.p. LPS + NOX2-I). Differences between NOX2$^{+/+}$ mice and NOX2$^{-/-}$ mice, as well as between NOX2$^{+/+}$ mice and NOX2$^{+/+}$ treated with NOX2-I, were analyzed separately using ANOVA with *post hoc* tests.

expression was attenuated in NOX2$^{-/-}$ mice with sepsis. In our model of systemic LPS injection, lack of neutrophilic NOX2 function will not contribute to bacteria-mediated neutrophil influx. However, NOX2 deficiency in the microvasculature may attenuate ICAM-1 expression and ICAM-1–mediated neutrophil influx. Others have shown that, consistent with our data, systemic sepsis or systemic viremia-induced lung injury in rodents is attenuated by chemical quenching of ROS or p47*phox* deficiency (33, 34). In summary, NOX2 appears to play a complex cell-type–specific role in sepsis-induced lung inflammation, with neutrophilic NOX2 necessary for bacterial clearance but with microvascular NOX2 activation contributing to lung inflammation. Experiments in mice with cell-type–specific NOX2 deficiency are necessary to dissect the dual role of NOX2 in sepsis.

During sepsis, bacterial ligands such as LPS engage TLRs and activate proinflammatory signaling, resulting in the activation of transcription factors NF-κB and AP-1 (12, 30, 32). Our results show that intraperitoneal LPS robustly activates IKK-β and MAPK (p38 and JNK) phosphorylation in the developing lung, and NOX2 deficiency inhibits canonical TLR pathway signaling. Although oxidative stress–mediated activation of protein kinase C, phospholipase 2 activation, and tyrosine phosphorylation have been reported before, the mechanisms underlying redox regulation of kinase activity in sepsis remain unclear (32, 33, 35–37). To investigate the mechanisms by which NOX2 regulates LPS-induced lung inflammation, we examined whether activation of proinflammatory TLR pathway kinases is NOX2 dependent in the developing lung. Our data showing that NOX2 regulates lung IKK-β and MAPK (p38 and JNK) phosphorylation in sepsis supports the possibility of a mechanism by which cellular redox status, via NOX enzymes, regulates innate immune signaling via TLRs. These *in vivo* data are consistent with studies from our group showing attenuation of LPS-mediated IKK-β phosphorylation with NOX2 silencing in lung endothelial cells (15). Induction of IKK-β and MAPK phosphorylation with sepsis was associated with nuclear localization of the p65 and c-Jun subunits of NF-κB and AP-1, supporting pulmonary

activation of transcription factors. NF-κB and AP-1 activation in sepsis was also evident in NOX2$^{-/-}$ mouse pups but it was significantly attenuated compared with NOX2$^{+/+}$ mice. Although consistent with the findings of studies reporting ROS-dependent activation of NF-κB and AP-1 during sepsis-induced lung injury, our data suggest that NOX2 regulates LPS-mediated activation of redox-sensitive transcription factors in the developing lung (38–42). ROS generated from the mitochondrial transport chain, uncoupled endothelial nitric oxide synthase, and xanthine oxidase have been reported to propagate lung inflammation during sepsis (10, 43). NOX2-derived superoxide can also interact with catalytic products of the above enzymes to form highly reactive ROS such as peroxynitrite, which contribute to inflammation and tissue damage (10, 14). Although our data confirm the role of NOX2 in lung inflammation and alveolar remodeling, future studies to dissect the cross-talk between NOX2 and other redox pathways in our model are planned. We used whole-lung tissue for our experiments and therefore are not able to discern the cell-type–specific role of NOX2 in sepsis-induced lung inflammation. Because NOX2 is expressed in multiple lung cell types, we sought to investigate the global effect of NOX2 loss or suppression (gp91*phox* ds-*tat*) on LPS-induced inflammation in the developing lung (18). Future studies will investigate the differential role of cell-type–specific NOX2 function in sepsis. These data provide new insights into the mechanisms by which NOX2 regulates proinflammatory TLR signaling during sepsis *in vivo*.

Animal models to study the effects of noxious stimuli on lung development in BPD have focused on prenatal endotoxin exposure, postnatal hyperoxia or hypoxia, and mechanical ventilation (20, 21, 44). To the best of our knowledge, this is one of the first studies to examine the mechanisms underlying systemic sepsis-induced lung remodeling, which is observed in premature infants who develop " new BPD" without significant exposure to hyperoxia or ventilation (2). In our model, LPS-induced inflammation in the developing lung results in increased mean linear intercepts and decreased radial alveolar counts, suggesting that systemic sepsis alone causes alveolar simplification (1). Our data are in agreement with studies showing that

intraamniotic endotoxin or neonatal intratracheal LPS exposures remodel the lung in rodents (45, 46), and suggest that activation of proinflammatory TLR signaling in the developing lung disrupts lung morphogenesis. Consistent with this postulate, NOX2$^{-/-}$ mice reveal decreased TLR-mediated lung inflammation and less alveolar simplification when compared with NOX2$^{+/+}$ mice after sepsis. Although lung matrix remodeling is a complex process in the developing lung, activation of MMPs in the setting of decreased levels of TIMP is a known cause of inflammation-dependent lung matrix degradation (47). We observed that lung MMP-9 levels increased with systemic LPS, with no change in TIMP-1 expression. Lung MMP-9 induction in sepsis was decreased in NOX2$^{-/-}$ mice, suggesting decreased alveolar destruction. Previous studies in premature infants have shown that increased MMP-9 or MMP-9/TIMP-1 levels are associated with increased risk of BPD (48, 49). Furthermore, in sepsis-related acute respiratory distress syndrome, imbalances in MMPs and their inhibitors, TIMPs, have been reported in animal studies as well as in humans (47, 50). To examine the relationship between sepsis-mediated alveolar simplification and pathways related to lung growth, we quantified FGF7 (keratinocyte growth factor) and elastin expression in our model (27, 28, 51). We found that LPS treatment decreased FGF7 and elastin expression in the lung, and that NOX2 deficiency attenuated this response. Differences in lung MMP-9 and FGF7 levels observed with sepsis might be potential mechanisms contributing to attenuated alveolar remodeling in NOX2$^{-/-}$ mice. Further research is required to understand the mechanisms underlying increased MMP-9 in sepsis and the function of NOX2 in regulating MMP-9 and TIMP-1 in the developing lung.

To test the potential therapeutic benefits of NOX2 inhibition on sepsis-induced lung inflammation, we performed experiments with gp91*phox* ds-*tat*, a cell-permeable peptide that inhibits NOX2 activation by disrupting assembly of the active NOX2 complex (31, 52). Data showing coimmunoprecipitation of p67*phox* with gp91*phox* 6 hours after systemic LPS demonstrate that an active NOX2 complex is assembled in the lung during sepsis. Pretreatment with gp91*phox*

ds-*tat* decreased coimmunoprecipitation of p67*phox* with gp91*phox*, confirming inhibition of lung NOX2 activation with the peptide inhibitor. Although the mechanism and specificity of gp91*phox* ds-*tat* has been elucidated *in vitro*, these original data validate its function *in vivo* (31, 53). Consistent with the inhibition of lung NOX2 assembly by gp91*phox* ds-*tat*, sepsis-induced cytokine and ICAM-1 expression were attenuated in mice treated with the peptide inhibitor. Furthermore, similar to our data obtained in NOX2$^{-/-}$ mice, gp91*phox* ds-*tat* decreased LPS-induced lung TLR pathway activation, as evidenced by decreased IKK-β/MAPK phosphorylation and NF-κB activation. Inhibition of proinflammatory TLR signaling with NOX2-I preserved lung architecture, as evidenced by increased radial alveolar counts and decreased mean linear intercepts. These data strongly suggest that NOX2 inhibition during neonatal sepsis attenuates lung inflammation, tissue damage, and alveolar remodeling. Although the use of gp91*phox* ds-*tat* in an animal model of sepsis is new, these data are consistent with other reports that indicate NOX2-mediated injury in hypertension, diabetes, and inflammasome activation is inhibited with gp91*phox* ds-*tat* (31, 54, 55). We used gp91*phox* ds-*tat* before intraperitoneal LPS injection to generate proof-of-principle data as a potential therapeutic agent in sepsis. Future studies must examine whether gp91*phox* ds-*tat* decreases lung inflammation if administered after LPS injection, and whether it is effective in the phase of sepsis caused by live bacteria.

Conclusions

In summary, we developed a model of systemic LPS injection in neonatal mice to investigate the mechanisms by which postnatal sepsis contributes to disrupted alveolar development. We demonstrated that systemic LPS administration activates canonical TLR signaling in the developing lung, which disrupts alveolar development, resulting in a phenotype similar to the alveolar simplification observed in premature infants with BPD. Using both genetic and inhibitor studies, we showed that NOX2 regulates proinflammatory TLR pathway activation in sepsis and that NOX2 deficiency or inhibition attenuates sepsis-induced lung injury and alveolar remodeling

in the developing lung. This study reveals the mechanisms by which a key enzyme family that regulates cellular redox signaling modulates lung innate immune function in sepsis. Investigating the effects of NOX2 manipulation on neonatal lung injury induced by live bacteria, as well as dissecting the cell-type–specific effects of NOX2 function in the pathophysiology of sepsis-induced lung inflammation and remodeling, are topics for future research. ■

References

1. Jobe AJ. The new BPD: an arrest of lung development. *Pediatr Res* 1999;46:641–643.
2. Kallapur SG, Jobe AH. Contribution of inflammation to lung injury and development. *Arch Dis Child Fetal Neonatal Ed* 2006;91:F132–F135.
3. Asikainen TM, Raivio KO, Saksela M, Kinnula VL. Expression and developmental profile of antioxidant enzymes in human lung and liver. *Am J Respir Cell Mol Biol* 1998;19:942–949.
4. Saugstad OD. Oxygen and oxidative stress in bronchopulmonary dysplasia. *J Perinat Med* 2010;38:571–577.
5. Vento M, Moro M, Escrig R, Arruza L, Villar G, Izquierdo I, Roberts LJ II, Arduini A, Escobar JJ, Sastre J, *et al*. Preterm resuscitation with low oxygen causes less oxidative stress, inflammation, and chronic lung disease. *Pediatrics* 2009;124:e439–e449.
6. Asikainen TM, White CW. Pulmonary antioxidant defenses in the preterm newborn with respiratory distress and bronchopulmonary dysplasia in evolution: implications for antioxidant therapy. *Antioxid Redox Signal* 2004;6:155–167.
7. Joung KE, Kim HS, Lee J, Shim GH, Choi CW, Kim EK, Kim BI, Choi JH. Correlation of urinary inflammatory and oxidative stress markers in very low birth weight infants with subsequent development of bronchopulmonary dysplasia. *Free Radic Res* 2011;45:1024–1032.
8. Davis JM, Parad RB, Michele T, Allred E, Price A, Rosenfeld W; North American Recombinant Human CuZnSOD Study Group. Pulmonary outcome at 1 year corrected age in premature infants treated at birth with recombinant human CuZn superoxide dismutase. *Pediatrics* 2003;111:469–476.
9. Pearson E, Bose C, Snidow T, Ransom L, Young T, Bose G, Stiles A. Trial of vitamin A supplementation in very low birth weight infants at risk for bronchopulmonary dysplasia. *J Pediatr* 1992;121:420–427.
10. Guo R-F, Ward PA. Role of oxidants in lung injury during sepsis. *Antioxid Redox Signal* 2007;9:1991–2002.
11. Shah J, Jefferies AL, Yoon EW, Lee SK, Shah PS; Canadian Neonatal Network. risk factors and outcomes of late-onset bacterial sepsis in preterm neonates born at < 32 weeks' gestation. *Am J Perinatol* 2015;32:675–682.
12. Akira S, Uematsu S, Takeuchi O. Pathogen recognition and innate immunity. *Cell* 2006;124:783–801.
13. Glaser K, Speer CP. Toll-like receptor signaling in neonatal sepsis and inflammation: a matter of orchestration and conditioning. *Expert Rev Clin Immunol* 2013;9:1239–1252.
14. Bedard K, Krause KH. The NOX family of ROS-generating NADPH oxidases: physiology and pathophysiology. *Physiol Rev* 2007;87:245–313.
15. Menden H, Tate E, Hogg N, Sampath V. LPS mediated endothelial activation in pulmonary endothelial cells: role of Nox2-dependent IKK-β phosphorylation. *Am J Physiol Lung Cell Mol Physiol* 2013:304:L445–L455.
16. Ogier-Denis E, Mkaddem SB, Vandewalle A. NOX enzymes and Toll-like receptor signaling. *Semin Immunopathol* 2008;30:291–300.
17. Patel DN, Bailey SR, Gresham JK, Schuchman DB, Shelhamer JH, Goldstein BJ, Foxwell BM, Stemerman MB, Maranchie JK, Valente AJ, *et al*. TLR4-NOX4-AP-1 signaling mediates lipopolysaccharide-induced CXCR6 expression in human aortic smooth muscle cells. *Biochem Biophys Res Commun* 2006;347:1113–1120.
18. Bernard K, Hecker L, Luckhardt TR, Cheng G, Thannickal VJ. NADPH oxidases in lung health and disease. *Antioxid Redox Signal* 2014;20:2838–2853.
19. Cardoso WV. Lung morphogenesis revisited: old facts, current ideas. *Dev Dyn* 2000;219:121–130.
20. Berger J, Bhandari V. Animal models of bronchopulmonary dysplasia. The term mouse models. *Am J Physiol Lung Cell Mol Physiol* 2014;307:L936–L947.
21. Hilgendorff A, Reiss I, Ehrhardt H, Eickelberg O, Alvira CM. Chronic lung disease in the preterm infant. Lessons learned from animal models. *Am J Respir Cell Mol Biol* 2014;50:233–245.
22. Coalson JJ. Pathology of bronchopulmonary dysplasia. *Semin Perinatol* 2006;30:179–184.
23. Sampath V, Davis K, Senft AP, Richardson TR, Kitzmiller JA, Berclaz PY, Korfhagen TR. Altered postnatal lung development in C3H/HeJ mice. *Pediatr Res* 2006;60:663–668.
24. Parkinson CM, O'Brien A, Albers TM, Simon MA, Clifford CB, Pritchett-Corning KR. Diagnostic necropsy and selected tissue and sample collection in rats and mice. *J Vis Exp* 2011;54:2966.
25. Cooney TP, Thurlbeck WM. The radial alveolar count method of Emery and Mithal: a reappraisal 2–intrauterine and early postnatal lung growth. *Thorax* 1982;37:580–583.
26. Knudsen L, Weibel ER, Gundersen HJ, Weinstein FV, Ochs M. Assessment of air space size characteristics by intercept (chord) measurement: an accurate and efficient stereological approach. *J Appl Physiol (1985)* 2010;108:412–421.
27. Bhandari A, Bhandari V. Biomarkers in bronchopulmonary dysplasia. *Paediatr Respir Rev* 2013;14:173–179.
28. Bland RD. Neonatal chronic lung disease in the post-surfactant era. *Biol Neonate* 2005;88:181–191.
29. O'Sullivan AW, Wang JH, Redmond HP. p38 MAP kinase inhibition promotes primary tumour growth via VEGF independent mechanism. *World J Surg Oncol* 2009;7:89.
30. Börgeling Y, Schmolke M, Viemann D, Nordhoff C, Roth J, Ludwig S. Inhibition of p38 mitogen-activated protein kinase impairs influenza virus-induced primary and secondary host gene responses and protects mice from lethal H5N1 infection. *J Biol Chem* 2014;289:13–27.
31. Cifuentes-Pagano E, Meijles DN, Pagano PJ. The quest for selective Nox inhibitors and therapeutics: challenges, triumphs and pitfalls. *Antioxid Redox Signal* 2014;20:2741–2754.
32. Gao X, Standiford TJ, Rahman A, Newstead M, Holland SM, Dinauer MC, Liu QH, Malik AB. Role of NADPH oxidase in the mechanism of lung neutrophil sequestration and microvessel injury induced by Gram-negative sepsis: studies in p47$^{phox-/-}$ and gp91$^{phox-/-}$ mice. *J Immunol* 2002;168:3974–3982.
33. Imai Y, Kuba K, Neely GG, Yaghubian-Malhami R, Perkmann T, van Loo G, Ermolaeva M, Veldhuizen R, Leung YH, Wang H, *et al*. Identification of oxidative stress and Toll-like receptor 4 signaling as a key pathway of acute lung injury. *Cell* 2008;133:235–249.
34. Liaw W-J, Chen TH, Lai ZZ, Chen SJ, Chen A, Tzao C, Wu JY, Wu CC. Effects of a membrane-permeable radical scavenger, Tempol, on intraperitoneal sepsis-induced organ injury in rats. *Shock* 2005;23:88–96.
35. Salomão R, Martins PS, Brunialti MK, Fernandes MdaL, Martos LS, Mendes ME, Gomes NE, Rigato O. TLR signaling pathway in patients with sepsis. *Shock* 2008;30:73–77.
36. Kuklin V, Kirov M, Sovershaev M, Andreasen T, Ingebretsen OC, Ytrehus K, Bjertnaes L. Tezosentan-induced attenuation of lung injury in endotoxemic sheep is associated with reduced activation of protein kinase C. *Crit Care* 2005;9:R211–R217.
37. Nagase T, Uozumi N, Aoki-Nagase T, Terawaki K, Ishii S, Tomita T, Yamamoto H, Hashizume K, Ouchi Y, Shimizu T. A potent inhibitor of cytosolic phospholipase A2, arachidonyl trifluoromethyl ketone, attenuates LPS-induced lung injury in mice. *Am J Physiol Lung Cell Mol Physiol* 2003;284:L720–L726.

38. Armstead VE, Opentanova IL, Minchenko AG, Lefer AM. Tissue factor expression in vital organs during murine traumatic shock: role of transcription factors AP-1 and NF-κB. *Anesthesiology* 1999;91: 1844–1852.

39. Feng X, Yan W, Liu X, Duan M, Zhang X, Xu J. Effects of hydroxyethyl starch 130/0.4 on pulmonary capillary leakage and cytokines production and NF-κB activation in CLP-induced sepsis in rats. *J Surg Res* 2006;135:129–136.

40. Guo R-F, Lentsch AB, Sarma JV, Sun L, Riedemann NC, McClintock SD, McGuire SR, Van Rooijen N, Ward PA. Activator protein-1 activation in acute lung injury. *Am J Pathol* 2002;161: 275–282.

41. Jarrar D, Kuebler JF, Rue LW III, Matalon S, Wang P, Bland KI, Chaudry IH. Alveolar macrophage activation after trauma-hemorrhage and sepsis is dependent on NF-κB and MAPK/ERK mechanisms. *Am J Physiol Lung Cell Mol Physiol* 2002;283:L799–L805.

42. Rahman I, Biswas SK, Jimenez LA, Torres M, Forman HJ. Glutathione, stress responses, and redox signaling in lung inflammation. *Antioxid Redox Signal* 2005;7:42–59.

43. Mittal M, Siddiqui MR, Tran K, Reddy SP, Malik AB. Reactive oxygen species in inflammation and tissue injury. *Antioxid Redox Signal* 2014;20:1126–1167.

44. D'Angio CT, Ryan RM. Animal models of bronchopulmonary dysplasia. The preterm and term rabbit models. *Am J Physiol Lung Cell Mol Physiol* 2014;307:L959–L969.

45. Benjamin JT, Smith RJ, Halloran BA, Day TJ, Kelly DR, Prince LS. FGF-10 is decreased in bronchopulmonary dysplasia and suppressed by Toll-like receptor activation. *Am J Physiol Lung Cell Mol Physiol* 2007;292:L550–L558.

46. Franco M-L, Waszak P, Banalec G, Levame M, Lafuma C, Harf A, Delacourt C. LPS-induced lung injury in neonatal rats: changes in gelatinase activities and consequences on lung growth. *Am J Physiol Lung Cell Mol Physiol* 2002;282:L491–L500.

47. Houghton AM. Matrix metalloproteinases in destructive lung disease. *Matrix Biol* 2015;44-46:167–174.

48. Bry K, Hogmalm A, Bäckström E. Mechanisms of inflammatory lung injury in the neonate: lessons from a transgenic mouse model of bronchopulmonary dysplasia. *Semin Perinatol* 2010;34: 211–221.

49. Fukunaga S, Ichiyama T, Maeba S, Okuda M, Nakata M, Sugino N, Furukawa S. MMP-9 and TIMP-1 in the cord blood of premature infants developing BPD. *Pediatr Pulmonol* 2009;44:267–272.

50. Ricou B, Nicod L, Lacraz S, Welgus HG, Suter PM, Dayer JM. Matrix metalloproteinases and TIMP in acute respiratory distress syndrome. *Am J Respir Crit Care Med* 1996;154:346–352.

51. Jankov RP, Keith Tanswell A. Growth factors, postnatal lung growth and bronchopulmonary dysplasia. *Paediatr Respir Rev* 2004;5 Suppl A:S265–S275.

52. Rey FE, Cifuentes ME, Kiarash A, Quinn MT, Pagano PJ. Novel competitive inhibitor of NAD(P)H oxidase assembly attenuates vascular O(2)(-) and systolic blood pressure in mice. *Circ Res* 2001;89:408–414.

53. Csányi G, Cifuentes-Pagano E, Al Ghouleh I, Ranayhossaini DJ, Egaña L, Lopes LR, Jackson HM, Kelley EE, Pagano PJ. Nox2 B-loop peptide, Nox2ds, specifically inhibits the NADPH oxidase Nox2. *Free Radic Biol Med* 2011;51:1116–1125.

54. Abais JM, Zhang C, Xia M, Liu Q, Gehr TW, Boini KM, Li PL. NADPH oxidase-mediated triggering of inflammasome activation in mouse podocytes and glomeruli during hyperhomocysteinemia. *Antioxid Redox Signal* 2013;18:1537–1548.

55. Sukumar P, Viswambharan H, Imrie H, Cubbon RM, Yuldasheva N, Gage M, Galloway S, Skromna A, Kandavelu P, Santos CX, *et al*. Nox2 NADPH oxidase has a critical role in insulin resistance-related endothelial cell dysfunction. *Diabetes* 2013;62: 2130–2134.